ELSEVIER

Journal of Chromatography A, 692 (1995) 319–325

JOURNAL OF CHROMATOGRAPHY A

Experimental evidence for the existence of duoselective (Type III) enantiomer separations in the capillary electrophoretic analysis of chiral weak acids

Mary E. Biggin[1], Robert L. Williams, Gyula Vigh*

Chemistry Department, Texas A&M University, College Station, TX 77843-3255, USA

Abstract

Experimental evidence has been found for the existence of the theoretically predicted *duoselective* (*Type III*) enantiomer separations in the capillary electrophoretic (CE) analysis of chiral weak acids. The mobilities of the enantiomers of 3,5-dinitrobenzamido phenylalanine were determined in the pH 3–6 range using constant ionic strength ϵ-amino-*n*-caproic acid background electrolytes and β-cyclodextrin as resolving agent. The complex formation constants and ionic mobilities of the free and complexed enantiomers were determined using the multiple equilibria-based electrophoretic mobility model. The extended peak resolution equation of CE was then used to calculate the peak resolution surfaces as a function of the pH and the β-cyclodextrin concentration of the background electrolyte, the dimensionless electroosmotic flow coefficient, and the effective portion of the applied potential. Though the observed peak resolution values were lower than predicted by the theory due to the presence of electromigration dispersion, the predicted and observed loci of the extrema of the resolution surface agreed well. The desionoselective/ionoselective/duoselective (DID) separation selectivity model and the peak resolution model permit the rational optimization of the CE separation of weak acid enantiomers.

1. Introduction

Capillary electrophoretic (CE) enantiomer separations have developed rapidly over the past few years, as demonstrated by a number of excellent, recent reviews [1,2]. Following an equilibrium model which rationalized such separations at constant pH as a function of the resolving agent concentration [3–5], an extended model was introduced to describe the effective mobilities (electroosmotic flow-corrected actual mobilities) of the enantiomers of weak electrolyte solutes as a function of both the pH and the chiral resolving agent concentration of the background electrolyte [6,7]. Specifically, the effective mobility of the *R*-enantiomer of a weak acid, μ_R^{eff}, was expressed as:

$$\mu_R^{eff} = \frac{\mu_-^0 + \mu_{RCD}^0 \cdot K_{RCD} \cdot [CD]}{1 + K_{RCD} \cdot [CD] + \frac{[H_3O^+]}{K_a}(1 + K_{HRCD}[CD])} \quad (1)$$

where μ_-^0 is the ionic mobility of the fully

* Corresponding author.

[1] Present address: Clarke College, Dubuque, IA 52002, USA.

0021-9673/95/$09.50
SSDI 0021-9673(94)01102-8

dissociated free enantiomer, $\mu^0_{RCD^-}$ is the ionic mobility of the fully dissociated complexed enantiomer, K_a is the acid dissociation constant of the enantiomer, K_{RCD^-} and K_{HRCD} are the formation constants for the complexes of the dissociated and non-dissociated forms of the enantiomer and the chiral resolving agent, cyclodextrin (CD), and $[H_3O^+]$ and [CD] are the hydronium and cyclodextrin concentrations, respectively. A similar expression was derived for the *S*-enantiomer. With these, separation selectivity, α, which was defined as the ratio of the effective mobilities of the two enantiomers:

$$\alpha = \frac{\mu_R^{eff}}{\mu_S^{eff}} \tag{2}$$

became:

$$\alpha = \frac{\mu^0_- + \mu^0_{RCD^-} K_{RCD^-}[CD]}{\mu^0_- + \mu^0_{SCD^-} K_{SCD^-}[CD]} \times \frac{1 + K_{SCD^-}[CD] + \frac{[H_3O^+]}{K_a}(1 + K_{HSCD}[CD])}{1 + K_{RCD^-}[CD] + \frac{[H_3O^+]}{K_a}(1 + K_{HRCD}[CD])} \tag{3}$$

Depending on the magnitude of the μ^0 and K values, three kinds of enantiomer separations were predicted [6,7]. In a *desionoselective* separation (previously called *Type I* separation [6,7]), $K_{RCD^-} = K_{SCD^-}$, $\mu^0_{RCD^-} = \mu^0_{SCD^-}$ and $K_{HRCD} \neq K_{HSCD}$, i.e. only the non-dissociated forms of the solutes complex selectively. This reduces the first term in Eq. 3 to unity and simplifies Eq. 3; in a *desionoselective* separation selectivity increases monotonously toward a limiting high value at low pH (below the pK_a) and high CD concentration.

In an *ionoselective* separation (previously called *Type II* separation [6,7]), $\mu^0_{RCD^-} \neq \mu^0_{SCD^-}$, $K_{RCD^-} \neq K_{SCD^-}$ and $K_{HRCD} = K_{HSCD}$, i.e. only the dissociated forms of the enantiomers complex selectively. The first and second terms in Eqn. 3 oppose each other, and $\alpha < 1$, $\alpha = 1$, and $\alpha > 1$ are all possible depending on the values of the parameters (μ^0 and K values) and the composition of the background electrolyte ($[H_3O^+]$ and [CD] values), allowing for — if so desired — the reversal of the migration order of the enantiomers.

In a *duoselective* separation (previously called *Type III* separation [6,7]), $\mu^0_{RCD^-} \neq \mu^0_{SCD^-}$, $K_{RCD^-} \neq K_{SCD^-}$ and $K_{HRCD} \neq K_{HSCD}$, i.e. both the dissociated and the non-dissociated forms of the enantiomers complex differently and $\alpha < 1$, $\alpha = 1$, and $\alpha > 1$ are again possible depending on the values of the parameters (μ^0 and K values) and the background electrolyte composition variables ($[H_3O^+]$ and [CD]). Thus, in a a *duoselective* separation the migration order of the enantiomers can be once again reversed if so desired.

In subsequent papers [8–10] an equation was derived for peak resolution as a function of separation selectivity, the effective charge of the enantiomers and the dimensionless electroosmotic flow:

$$R_s = \sqrt{\frac{Ele_0}{8kT}} \times \frac{\mathrm{abs}(\alpha - 1)\sqrt{\mathrm{abs}(\alpha + \beta)}\sqrt{\mathrm{abs}(1 + \beta)}\sqrt{z_R^{eff}}\sqrt{z_S^{eff}}}{\sqrt{\mathrm{abs}[(\alpha + \beta)^3]z_R^{eff}} + \sqrt{\alpha\,\mathrm{abs}[(1 + \beta)^3]z_S^{eff}}} \tag{4}$$

where E is the field strength, l the length of the capillary from injector to detector, e_0 the electric charge, k the Boltzman constant, and T the absolute temperature, z_R^{eff}, z_S^{eff} the effective charge of the enantiomers, and β the dimensionless electroosmotic flow coefficient defined as:

$$\beta = \frac{\mu_{eo}}{\mu_S^{eff}} \tag{5}$$

with

$$\mu_S^{obs} = \mu_S^{eff} + \mu_{eo} \tag{6}$$

where μ_S^{obs} is the observed mobility of the *S*-enantiomer, and μ_{eo} is the coefficient of the electroosmotic flow. This equation encompasses, as a limiting case, the R_s expression derived by Kenndler et al. in the absence of electroosmotic flow [11].

The effective charge of the *R*-enantiomer, z_R^{eff}, was expressed [8] as:

$$z_R^{eff} = \frac{z_-^0 + z_{RCD^-}^0 \cdot K_{RCD^-}[CD]}{1 + K_{RCD^-}[CD] + \frac{[H_3O^+]}{K_a}(1 + K_{HRCD}[CD])} \quad (7)$$

with z_-^0 and $z_{RCD^-}^0$ as the ionic charges of the fully dissociated enantiomer, non-complexed and complexed, respectively.

Since different selectivity surfaces belong to the different separation types, and since R_s depends on α and z^{eff}, there will be a unique peak resolution surface for each separation type [9,10]. *Desionoselective* separations will have a single lobe, while *ionoselective* separations and *duoselective* separations will have two lobes on their $R_s([H_3O^+], [CD])$ surfaces. Knowledge of the general shape of these surfaces is important for the rational optimization of the CE separation of the enantiomers of weak electrolytes.

Though three different enantiomer separation types were predicted theoretically, only *desionoselective* separations have been observed experimentally for chiral weak acids, either with β-cyclodextrin [6] or hydroxypropyl β-cyclodextrin [8], as resolving agent. The objective of this paper is to provide the first experimental evidence for the existence of *duoselective* separations in the CE analysis of monoprotic chiral weak acids.

2. Experimental

A P/ACE 2100 system (Beckman Instruments, Fullerton, CA, USA), operated at 210 nm and at a thermostatting liquid bath temperature of 37°C was used for the mobility measurements. The injector electrode was kept at ground potential, the detector electrode at high positive potential. The field strength was varied between 190 and 260 V/cm to keep the power dissipation around 100 mW. The 0.1–0.2 m*M* samples were injected electrokinetically. Benzyl alcohol, simultaneously injected at the detector end of the capillary, was used as electroosmotic flow marker. Untreated, 25 μm I.D., 150 μm O.D. (40.0 cm from injector to detector, 46.4 cm total length) fused-silica capillaries (Polymicro Technologies, Phoenix, AZ, USA) were used for the separations.

The background electrolytes (BGE) contained 0–15 m*M* β-cyclodextrin (American Maize Products, Hammond, IN, USA) as chiral resolving agent, 100 m*M* ϵ-amino-*n*-caproic acid, EACA, (Sigma, St. Louis, MO, USA) as buffer component, 100 m*M* methanesulfonic acid, MSA, (Aldrich, Milwaukee, WI, USA) as ionic strength adjusting agent and 250MHR PA hydroxyethyl cellulose, HEC, (Aqualon Company, Wilmington, DE, USA) as electroosmotic flow-controlling agent. The buffer pH was adjusted by a concentrated LiOH (Aldrich) solution. The test solute, 3,5-dinitrobenzamido phenylalanine (DPA), was synthesized according to a modified Schotten-Bauman procedure [12] from both racemic and enantiomerically pure phenylalanine (Aldrich) and 3,5-dinitrobenzoyl chloride (Fluka, Ronkonkona, NY, USA). In order to monitor the ionic strength-related mobility changes, a strong electrolyte, *p*-toluenesulfonic acid, PTSA (Aldrich), was added to each sample. All BGEs were freshly prepared using deionized water from a Millipore Q unit (Millipore, Milford, MA, USA). Irrespective of the pH of the BGE, the cation concentration was maintained constant at 100 m*M* (cation-concentration balanced background electrolytes [8–10]).

The parameters in Eqs. 1 and 4 and the three-dimensional selectivity and resolution surfaces were calculated from the measured, electroosmotic flow-corrected effective mobilities using the Origin Ver. 3.0 software package (MicroCal, Northampton, MA, USA) running on a 486DX2 66 MHz 16M RAM personal computer (Computer Access, College Station, TX, USA), as described in Refs. [8–10].

3. Results and discussions

3.1. Determination of the model parameters for 3,5-dinitrobenzamido phenylalanine

The K_a and μ_-^0 values of the weak acid test solute, DPA, were determined using the counterion concentration-balanced BGEs in the pH 3–6

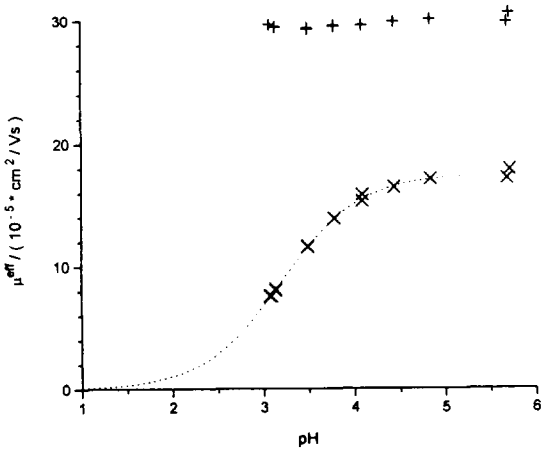

Fig. 1. Effective mobility of $PTSA^-$ (symbol +) and DPA^- (symbol ×) in 100 m*M* ε-amino-*n*-caproic acid, 100 m*M* methanesulfonic acid buffers as a function of the BGE pH value, adjusted by lithium hydroxide.

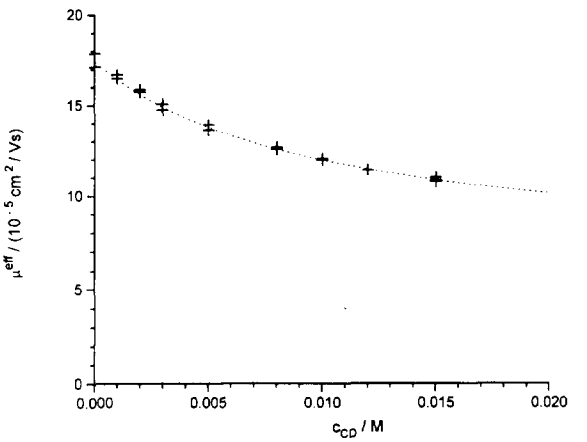

Fig. 2. Effective mobility of the less mobile enantiomer of DPA^- (symbol +) as a function of the β-cyclodextrin concentration in pH 5.68 counter-ion concentration balanced 100 m*M* EACA BGEs.

range. The effective mobilities of DPA (symbol ×) and PTSA (symbol +) are plotted in Fig. 1 as a function of pH. The mobilities of the permanent anion, $PTSA^-$, are indeed constant — within experimental scatter — in the counter-ion concentration balanced BGEs indicating that the μ^{eff} values of the enantiomers are suitable for the pK_a and μ^0_- determinations [8]. The calculated K_a and μ^0_- values of DPA are listed in Table 1.

In order to determine the $\mu^0_{RCD^-}$, $\mu^0_{SCD^-}$, K_{RCD^-} and K_{SCD^-} values, listed in Table 1, the concentration of β-cyclodextrin was varied between 0 and 15 m*M* in pH = 5.68 BGEs where DPA is almost completely dissociated, and the effective mobilities as a function of c_{CD} were measured (Fig. 2). Next, the K_{HRCD} and K_{HSCD} values were determined from the effective mobilities measured in pH = 3.08 BGEs (where DPA is less than 50% dissociated) as c_{CD} was varied between 0 and 15 m*M* (Fig. 3). The calculated constant values are listed in Table 1.

Since $\mu^0_{RCD^-} = 5.82 \cdot 10^{-5}$ cm^2/Vs and $\mu^0_{SCD^-} = 6.53 \cdot 10^{-5}$ cm^2/Vs, $K_{RCD^-} = 62$ and $K_{SCD^-} = 100$, and $K_{HRCD} = 62.7$ and $K_{HSCD} = 81.1$, the separation of the enantiomers of DPA represents a *duoselective* separation. To the best of our

Table 1
Estimated model parameter values for DPA

μ^0_- (10^{-5} cm^2/Vs)	17.49 ± 0.09
$10^4 K_a$	6.4 ± 0.1
pK_a	3.19
$\mu^0_{RCD^-}$ (10^{-5} cm^2/Vs)	6.5 ± 0.4
$\mu^0_{SCD^-}$ (10^{-5} cm^2/Vs)	5.8 ± 0.8
$K^0_{RCD^-}$	100 ± 7
K^0_{SCD}	62 ± 7
K_{HRCD}	81.1 ± 0.8
K_{HSCD}	62.7 ± 0.5

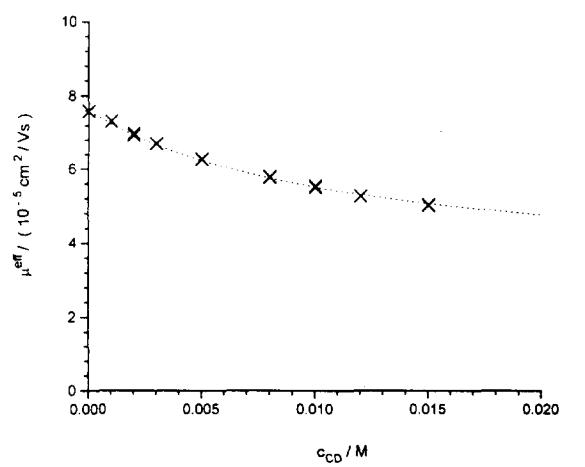

Fig. 3. Effective mobility of the less mobile enantiomer of DPA^- (symbol ×) as a function of the β-cyclodextrin concentration in pH 3.08 counter-ion concentration balanced 100 m*M* EACA BGEs.

knowledge, this is the first, experimentally demonstrated example of a *duoselective* CE separation of a chiral weak acid.

3.2. Separation selectivity and peak resolution surfaces

Once the model parameters are known, the selectivity and resolution surfaces can be calculated and studied to understand the behavior of a *duoselective* weak acid separation and to find the conditions which lead to optimum peak resolution. The selectivity surface is shown in Fig. 4 as a function of c_{CD} and pH. At high pH (pH > $pK_a + 1$), selectivity passes a maximum value as c_{CD} is varied: the maximum is located at 15 m*M*. Fortunately, the surface is sufficiently flat in the $10 < c_{CD} < 20$ m*M* range, which leads to rugged separations. If one keeps the CD concentration constant at $c_{CD} = 15$ m*M* and begins to decrease the pH from 6, α first remains constant, then begins to decrease in the vicinity of the pK_a. Upon further decrease of the pH, α becomes less than unity, indicating that the migration order of the enantiomers is reversed. Simultaneously, as the pH is decreased, the locus of α_{max} shifts toward lower cyclodextrin concentrations. This follows the predicted typical behavior of a *duoselective* separation [6].

The calculated peak resolution surface is shown in Fig. 5. Since resolution depends on the magnitude of the electroosmotic flow as well (expressed here as β), its value has to be fixed for the calculations. With uncoated fused-silica capillaries, the electroosmotic flow works against the migration of the anionic solutes. However, in these measurements, its magnitude was kept low by the addition of HEC. Therefore, the surface in Fig. 5 was calculated with $\beta = 0$. There are two lobes on the resolution surface: the primary lobe is at high pH, and the migration order of the enantiomers is D first, L second. The secondary lobe is at low pH, and there the migration order of the enantiomers is L first, D second. The two lobes are separated by a valley, where the resolution is zero. At high pH, on the primary lobe, resolution is high and the resolution maximum on the fortunately flat R_s surface is in the $12 < c_{CD} < 18$ m*M* range. If one keeps the CD concentration constant at 15 m*M* and moves toward lower pH values, R_s drops precipitously around the pK_a value. There are

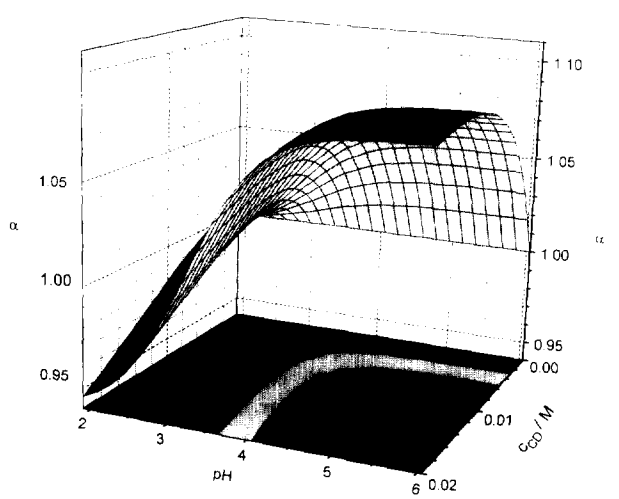

Fig. 4. Selectivity surface for the separation of the enantiomers of DPA^- (duoselective separation) as a function of the β-cyclodextrin concentration and the pH in counter-ion concentration balanced 100 m*M* EACA BGEs. The surface was calculated with Eq. 3 and the constants in Table 1.

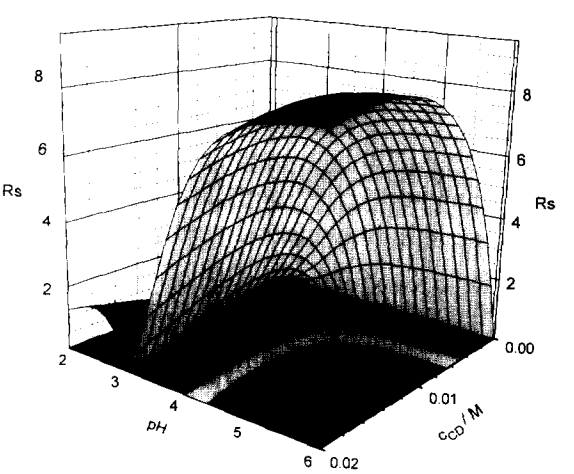

Fig. 5. Peak resolution surface for the separation of the enantiomers of DPA^- (duoselective separation) as a function of the β-cyclodextrin concentration and the pH in counter-ion concentration balanced 100 m*M* EACA BGEs. The surface was calculated with Eq. 4 and the constants in Table I for $\beta = 0$ and $E = 215$ V/cm, $T = 298$ K and $l = 38.65$ cm.

two factors which cause this rapid loss of resolution: the loss of selectivity shown in Fig. 4, and the accompanying loss in effective solute charge (cf. Eq. 3). As pH is decreased further, resolution is increased again, albeit with a reversed peak migration order. Even though selectivity keeps increasing as pH is lowered further (cf. Fig. 4), R_s goes through a maximum, because the loss of effective charge overcompensates the selectivity gain. This surface agrees with what was predicted theoretically as typical for a *duoselective* separation and indicates that reasonably rugged separations can be achieved as long as the pH is kept at least one pH unit above the pK_a. Above this limit, the pH can be selected freely to accommodate other considerations.

In order to demonstrate how closely the predicted values agree with the measured ones, another series of experiments was carried out in which the pH of the counter-ion concentration-balanced 100 m*M* EACA BGE was varied between 3 and 5.8, and the β-cyclodextrin concentration was kept at 15 m*M*. The selectivity values are plotted in Fig. 6 (symbol × measured values, solid line, calculated values), indicating that the agreement is excellent. The predicted (symbol ×) and measured (symbol +) R_s values for the same set of experiments are shown in Fig.

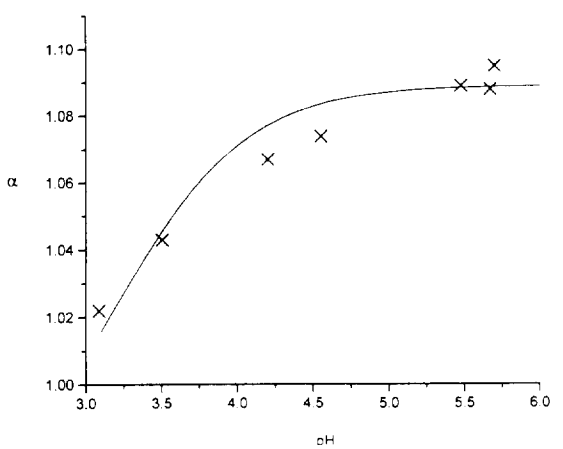

Fig. 6. Comparison of the predicted (solid line) and measured (symbol ×) selectivity values for DPA as a function of pH in counter-ion concentration balanced 100 m*M* EACA, 15 m*M* β-cyclodextrin BGEs.

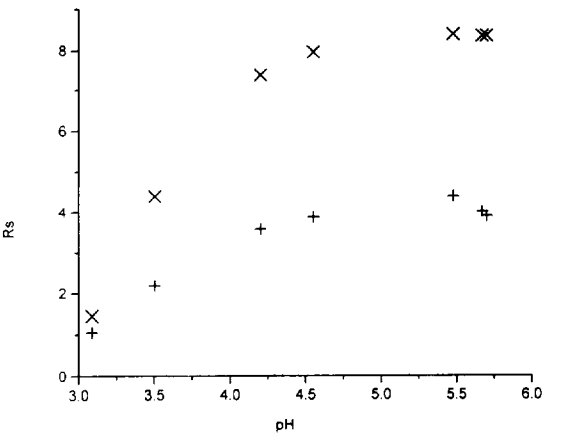

Fig. 7. Comparison of the predicted (symbol ×) and measured (symbol +) R_s values for DPA^- as a function of pH in counter-ion concentration balanced 100 m*M* EACA, 15 m*M* β-cyclodextrin BGEs. The measured values were obtained using $E = 215$ V/cm, with electroosmotic flows varying in the $(0.2–0.4)\cdot 10^{-5}$ cm^2/Vs range.

7. Though the measured values are about 50% smaller than the theoretically predicted ones (indicating the presence of additional peak broadening mechanisms in excess of longitudinal diffusion considered in the derivation of Eq. 4), the loci of the experimental and theoretical peak resolution maxima agree well, indicating that the model is suitable for the selection of the operating conditions which lead to maximum resolution of the enantiomers. As an example, the electropherogram of a DPA sample is shown in Fig. 8.

4. Conclusions

The multiple equilibria-based mobility model of CE was used to determine the complex formation constants and ionic mobilities in the CE separation of the enantiomers of a weak acid, DPA. The numeric values of the constants indicate that this separation represents a *duoselective* separation, and serves as the first experimental evidence for the existence of this theoretically predicted separation possibility. The model parameters and the extended peak resolution equation were used to calculate the

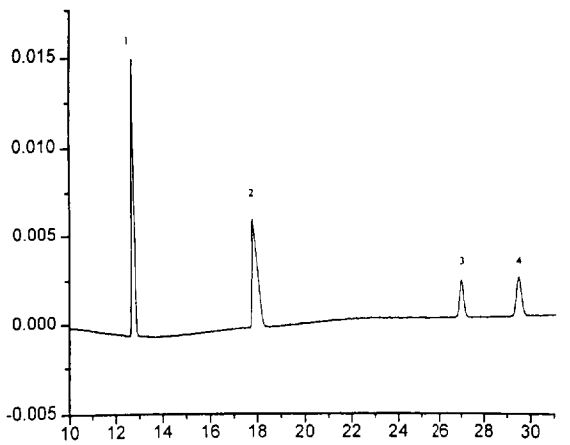

Fig. 8. Electropherogram of a DPA sample, obtained in a counter-ion concentration balanced 100 m*M* EACA, pH = 5.69, 15 m*M* β-cyclodextrin BGE. $E = 215$ V/cm at $T = 310$ K. Peak identity: 1 = $PTSA^-$, 2 = 3,5-dinitrobenzoic acid, 3 and 4 = DPA enantiomers. *x*-axis: time (min); *y*-axis: absorbance (mAU).

predicted peak resolution surface for the enantiomers, which was then compared to the experimentally determined values. Though the actual peak resolution values were lower than the theoretically predicted ones due to the presence of additional peak broadening mechanisms other than longitudinal diffusion, the loci of the peak resolution extrema agreed with the theoretical predictions, indicating that the model can be used for the selection of the operating conditions which lead to maximum resolution of the enantiomers.

Acknowledgements

Partial financial support by the National Science Foundation (CHE-8919151 and an NSF-REU fellowship to M.E.B.), the Texas Coordination Board of Higher Education Advanced Research Program (Project Number 010366-016), Beckman Instruments (Fullerton, CA, USA), the WR Johnson Pharmaceutical Research Institute (Springfield, PA, USA), and the Dow Chemical Company (Midland, MI, USA) is gratefully acknowledged. American Maize Products Corporation (Hammond, IN, USA) and the Aqualon Corporation (Wilmington, DE, USA), respectively, are acknowledged for the donation of the β-cyclodextrin and hydroxyethyl cellulose samples.

References

[1] R. Kuhn and S. Hoffstetter-Kuhn, *Chromatographia*, 34 (1992) 505.
[2] J. Snopek, I. Jelinek and E. Smolkova-Keulemansova, *J. Chromatogr.*, 609 (1992) 1.
[3] S.A.C. Wren and R.C. Rowe, *J. Chromatogr.*, 603 (1992) 235.
[4] S.A.C. Wren and R.C. Rowe, *J. Chromatogr.*, 609 (1992) 363.
[5] S.A.C. Wren and R.C. Rowe, *J. Chromatogr.*, 635 (1993) 113.
[6] Y.Y. Rawjee, D.U. Staerk and Gy. Vigh, *J. Chromatogr.*, 635 (1993) 291.
[7] Y.Y. Rawjee, R.L. Williams and Gy. Vigh, *J. Chromatogr A.*, 652 (1993) 233.
[8] Y.Y. Rawjee and Gy. Vigh, *Anal. Chem.*, 66 (1994) 619.
[9] Y.Y. Rawjee, R.L. Williams and Gy. Vigh, *J. Chromatogr. A*, 680 (1994) 599.
[10] Y.Y. Rawjee, R.L. Williams, L. Buckingham and Gy. Vigh, *J. Chromatogr. A*, 688 (1994) 273.
[11] W. Friedl and E. Kenndler, *Anal. Chem.*, 65 (1993) 2003.
[12] P.L. Camacho, Gy. Vigh and D.H. Thompson, *J. Chromatogr.*, 641 (1993) 31.